Universal Journal of Renewable Energy **9 (2021), 25-39**
www.papersciences.com **EU Academy of Sciences (EUAS) e-Symposium**

Recent Progress and Perspective in N-doped Carbon-based Anodes for Potassium Ion Batteries

Q. Jiang
Key Laboratory of Automobile Materials, Ministry of Education & School of Materials Science and Engineering, Jilin University
Changchun 130022, China
jiangq@jlu.edu.cn

Abstract
The ever-increasing demand for eco-friendly and large-scale energy storage systems requires novel rechargeable batteries beyond lithium-ion batteries (LIBs) which is severely hindered by the insufficient lithium resources. In this regard, potassium ion batteries (PIBs) have attracted extensive attention owing to their earth sufficiency, low cost and similar charge storage mechanism to LIBs. However, the research on PIBs is still in infancy and the identification of appropriate anode materials is imperative. Carbon-based materials have become one of the most promising anodes for PIBs thanks to their advantages of abundance, nontoxicity and security. In addition, heteroatoms doping, particularly N-doping, in carbon materials is an efficient method to afford numerous electrochemical active sites and to promote the ion/electron transport rate, thus enhancing their electrochemical performances. Herein, we provide a minireview on N-doped carbon-based anode materials for PIBs, covering the potassium storage mechanisms, evolution of the PIBs, synthetic routes and recent achievements, as well as their advantages/disadvantages. This review may provide a practical guidance to explore high-performance low-cost anodes to improve the feasibility of PIBs.

Key Word and Phrases
N-doping, Carbon-based Materials, Potassium Ion Batteries, Electrochemical Performances.

1. Introduction

In the past few decades, with increasing consumption of fossil fuels and serious environmental problems, renewable and clean energies have been considered as the most important material basis for human survival and development [1], [2]. Solar, wind and geothermal energies, etc. are regarded as the renewable and eco-friendly energy sources, however, they are inherently intermittent and seasonal [3], [4]. Therefore, energy storage devices play a key role to store and deliver these intermittent energies [5]. Among existing energy storage systems, lithium ion batteries (LIBs) have been considered as the dominant electrochemical energy storage devices and become indispensable for sustaining daily life thanks to the advantages of convenience, high energy density, long life and lack-of-memory property [6], [7]. However, the scarcity and uneven distribution of lithium resource suggest a gloomy outlook for the large-scale application of LIBs [8], [9]. These challenges inspire extensive studies on alternative, sustainable, and affordable battery technologies, such as sodium ion batteries (SIBs), potassium ion batteries (PIBs), zinc ion batteries, magnesium ion batteries, aluminum ion batteries, etc. [10]-[14].

As the same main group elements in the periodic table, sodium and potassium have similar physical and chemical properties to lithium, making SIBs and PIBs promising alternatives to LIBs thanks to the abundant reserve and low cost of sodium and potassium resources [15], [16]. In comparison to LIBs and SIBs, PIBs possess three significant strengths. First, the redox potential of K/K^+ (-2.93 V *vs.* the standard hydrogen electrode, SHE) is lower than that of Na/Na^+ (-2.71 V *vs.* SHE) and is closer to that of Li/Li^+ (-3.04 V *vs.* SHE). This enables PIBs to have higher discharge voltage plateau and energy density than SIBs [17]. More importantly, the greatest advantage of PIBs over SIBs is that the commercial graphite can form the graphite intercalation compound KC_8 with a theoretical capacity of 279 mAh g^{-1}, which is a considerable value compared to that of LIBs (372 mAh g^{-1}) [18]. While SIBs only offer a discharge capacity of 35 mAh g^{-1} by forming NaC_{64}

[19]. In addition, it is reported that electrolytes in PIBs exhibit higher conductivity than those in LIBs and SIBs, which is attributed to the weaker Lewis acidity and the corresponding smaller Stokes radius of solvated K^+ [20], [21]. Furthermore, potassium does not form alloy with cheaper Al current collector (rather than Cu), which could reduce the production cost of the cells [22]. Taken these advantages together, PIBs have rapidly attracted broad attention and been considered as one of the most promising alternative next-generation energy storage techniques. Similar to LIBs, PIBs exhibit a typical rocking-chair working mechanism on battery operation, as demonstrated in Fig. 1 [based on Prussian blue analogues as cathode, graphite as anode, and KPF_6/ethylene carbonate (EC): diethyl carbonate (DEC) as electrolyte] [23]. K^+ shuttles between the cathode and the anode. During the charging process, K^+ deintercalates from the active material in cathode, passes through the electrolyte and finally intercalates into the active materials in anode. While during the discharging process, the reverse reaction occurs, *i.e.* the inserted K^+ in the anode is extracted and reinserted into the cathode, accompanied with the electrons transfer through the external circuit. However, the larger ionic radius of K^+ (1.38 Å), compared to Li^+ (0.68 Å) and Na^+ (0.97 Å), makes it difficult for the diffusion of K^+ in host materials as well as leads to a large expansion during K^+ insertion/extraction. Therefore, it is urgently required to optimize PIBs host materials to allow effective and rapid reversible K^+ insertion/extraction.

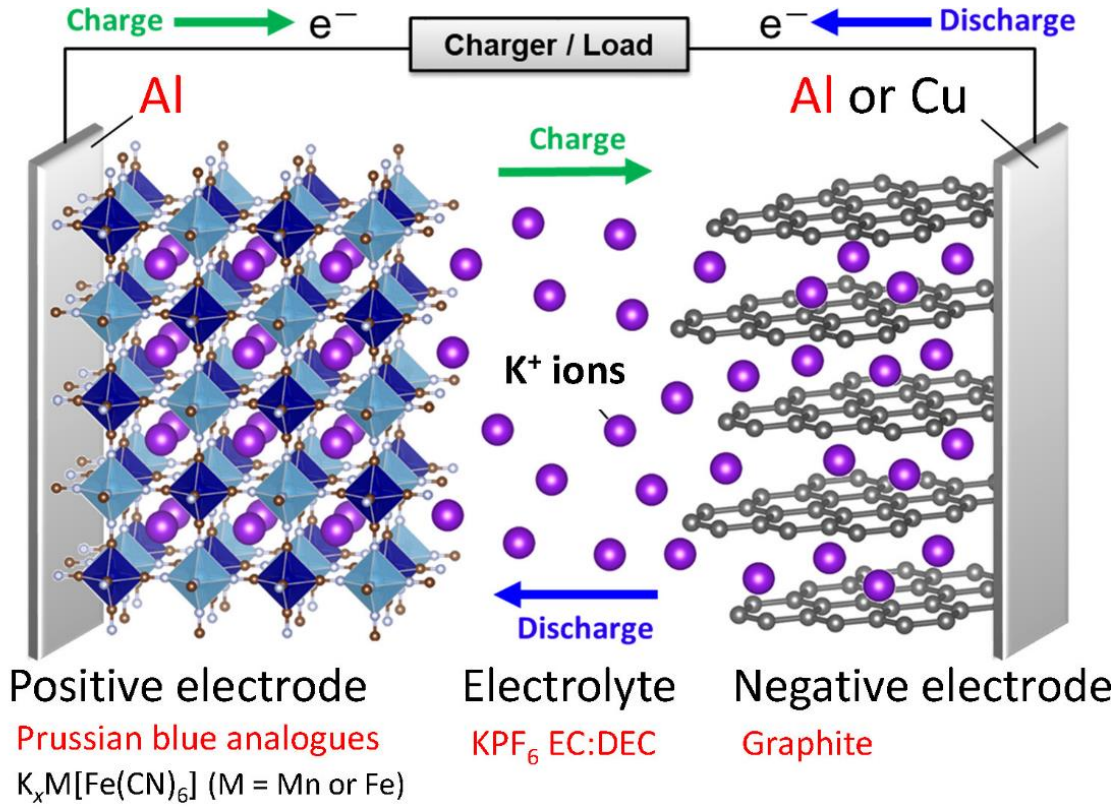

Fig. 1 Schematic illustration of the cell configuration and operational mechanism of a typical PIB.[23] Copyright 2020, American Chemical Society.

According to the reaction mechanism, PIBs anodes contain three types: intercalation mechanism, such as carbonaceous and titanium-based materials [24], [25]; conversion mechanism, containing metal oxides, sulfides and selenides [26], [27]; and alloying mechanism, including tin (Sn), bismuth (Bi), antimony (Sb) and phosphorous (P) [28]-[31]. Among them, carbon-based materials have been widely investigated thanks to the abundance, nontoxicity, high electrical conductivity and chemical stability. However, carbon-based materials are limited by the low theoretical capacities and sluggish kinetics during rapid K^+ insertion/extraction. To address these challenges, extensive efforts have been devoted, significantly improving the electrochemical

performances of PIBs. There into, heteroatoms (such as N, O, S and P) doping, can generate plenty of defects for K^+ adsorption, thus enhancing the comprehensive electrochemical performance of carbon materials. Among them, N-doping is the most studied one, which can enhance the electronic conductivity and reaction activity by generating abundant extrinsic defects.

In this review, we discussed the possible potassium storage mechanism of N-doped carbon-based materials (including graphitic carbons and non-graphitic carbons), synthetic routes and important progresses. Finally, the critical issues, challenges, and perspectives are presented to provide a guidance for the future research direction of PIBs.

2. A brief History of Carbon Anodes for PIBs

Since the 1950s, the K-graphite intercalated compounds (K-GIC) have been reported in literatures [32], [33]. However, their electrochemical performances were studied later. Ji *et al*. [34] for the first time reported electrochemical potassium insertion in graphite in a nonaqueous electrolyte, which can exhibit a high reversible capacity of 273 mAh g^{-1}. Graphite materials possess obvious layer stacking structure, and their potassium storage comes from the intercalation of K^+ on graphitic layers. The potassium storage mechanism in graphite for the selected states of discharge/charge in the first cycle were investigated by the ex-situ X-ray diffraction (XRD) (see Fig. 2). Upon potassiation, KC_{36} (point 4) was first observed between 0.3 and 0.2 V while graphite diffraction peaks vanish. As the potassiation exceeds, KC_{36} further transforms to KC_{24} (point 5) between 0.2 and 0.1 V. Finally, KC_8 was converted near 0.01 V (point 6 and 7). While during the depotassiation process, KC_8 was replaced by KC_{36} (point 11) around 0.3 V, while KC_{24} was not detected. Finally, a broad peak of graphite reappeared at above 0.5 V (point 12 and 13), manifesting the highly reversible process. In order to further illustrate the electrochemical behavior, Luo *et al*. [35] also studied the potential phases for K^+ intercalation into graphite by density functional theory (DFT) simulations (see Fig. 3). Different from SIBs, the storage mechanism of carbon-based anodes in PIBs is more similar to that in LIBs. It proposed a different three-step inserted process of K^+ into graphite: C → KC_{24} (stage III) → KC_{16} (stage II) → KC_8 (stage I). DFT simulations also showed that KC_8 was the maximum stable stoichiometry. Compared with the investigation of Ji *et al*., this study showed the same fully discharged product (KC_8) only with different intermediate phases during the discharge process.

Although the electrochemically reversible potassium storage in graphite has been experimentally confirmed, the electrochemical performance in terms of capacity, cyclability, and rate capability is still unsatisfied. Therefore, various anodes, especially carbon-based materials, have been successfully explored and applied in PIBs systems. All these efforts are greatly pushing forward the development of PIBs.

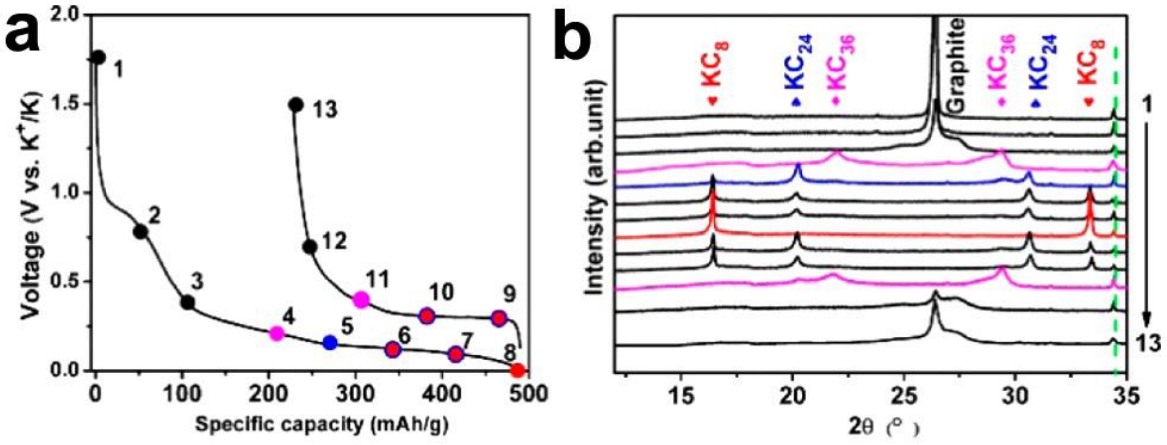

Fig. 2 (a) Charge/discharge potential profiles of a graphite electrode in nonaqueous PIBs. (b) *Ex-situ* XRD patterns of a graphite electrode at selected charge/discharge states.[34] Copyright 2015, American Chemical Society.

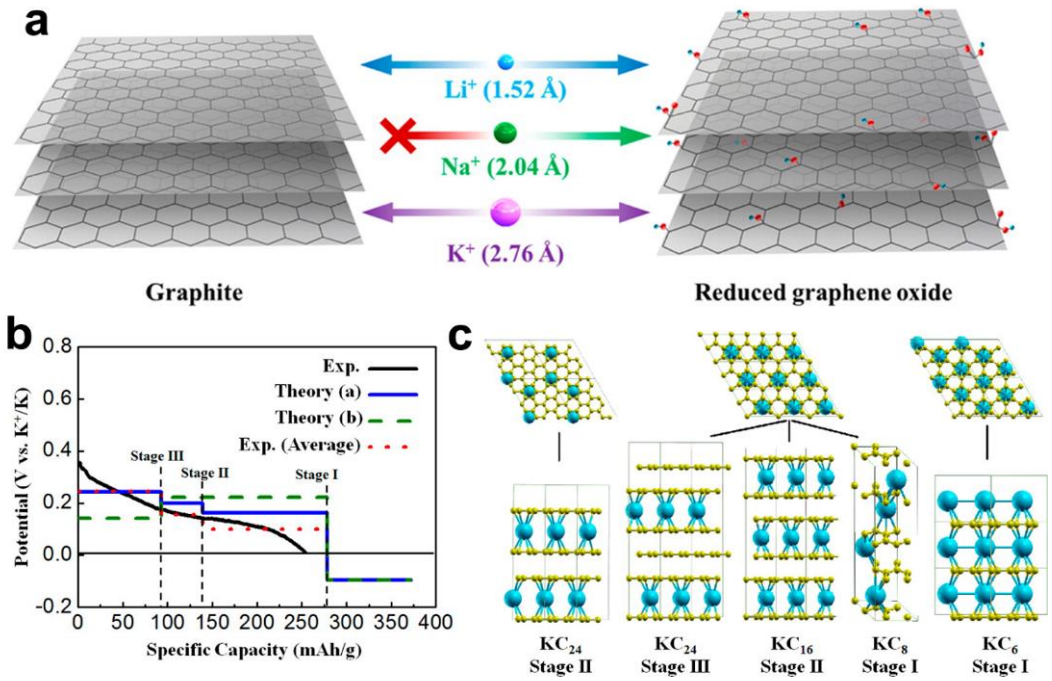

Fig. 3 (a) Schematic illustration of electrochemical intercalation of Li^+, Na^+, and K^+ into graphite and reduced graphene oxide (rGO). (b) Calculated potential profile for K^+ intercalation into graphite for different staging scenarios. Blue line (Theory (a)) corresponds to an intercalation staging: KC_{24} (Stage III) → KC_{16} (Stage II) → KC_8 (Stage I). Green dotted line (Theory (b)) corresponds to calculated values for the previously reported staging: KC_{24} (Stage II) → KC_8 (Stage I). Red dotted line corresponds to the averaged experimental data shifted by 26 mAh g^{-1} to correct the capacity contribution from SEI formation. (c) Scheme of the different stages of K-intercalated graphite, K shown in blue and C in yellow.[35] Copyright 2015, American Chemical Society.

3. Advanced N-doped Carbon Materials

Carbon materials have been widely investigated and employed as anodes in PIBs thanks to their abundance, low cost, and stability. Carbon materials are commonly in forms of graphite, graphene, hard carbon materials and soft carbon, which can be divided into graphitic carbon and non-graphitic carbon.

3.1 N-doped Graphitic Carbon

Compared with graphite anodes, graphene materials possess a better potassium storage since K^+ can be adsorbed on two sides of the graphene layer. The potassium storage of N-doped graphene is mainly from K^+ absorption on the surface, including the defects and functional groups. Luo and co-workers [35] reported the potassium storage performances of rGO film. Thanks to the plentiful surface groups of rGO, it shows a relatively higher capacity than the graphite anode. However, the electrochemical performance was still not satisfied. Recent studies demonstrated that the electrochemical properties of graphene can be enhanced via N-doping [36], [37]. For instance, Share *et al*. [36] found that N-doped few-layered graphene (N-FLG) possessed a capacity of 350 mAh g^{-1}, higher than that of graphite (theoretical capacity of 279 mAh g^{-1}). The enhancement of the storage capacity mainly comes from the optimal electronic structure and increased active sites thanks to the introducing of N heteroatom into the graphite lattice. Particularly, from *in-situ* Raman spectroscopy, they also found that defects sites might hinder the formation of K-GIC, but N-doped sites could sustain KC_8 formation and provide extra capacity (see Fig. 4). In addition, Ju *et al*. [37] also successfully prepared few-layer N-doped graphene (FLNG) with high N content (14.68 at%) by a simple bottom-up synthesis method using dicyandiamide and coal tar pitch as precursors. The FLNG electrode contains a considerable reversible capacity (320 mAh g^{-1} at 0.05 A g^{-1} after 60 cycles), superior rate capability (170 mAh g^{-1} at 500 mA g^{-1}), as well as long-term cycling life at a

relatively higher discharge current density (150 mAh g^{-1} at 0.5 A g^{-1} after 500 cycles). On one hand, N-doping can improve the conductivity of the FLNG, which is conductive to achieve competitive rate performance and cycle stability. On the other hand, N-doping can activate the distributed reversible storage sites in the graphene lattice and maintain the energetic pathway for the formation of KC_8. Some progresses of electrochemical performances have been made by N-doping, however, the practical application of graphene anodes is still challenged due to the huge volume change during the electrochemical process.

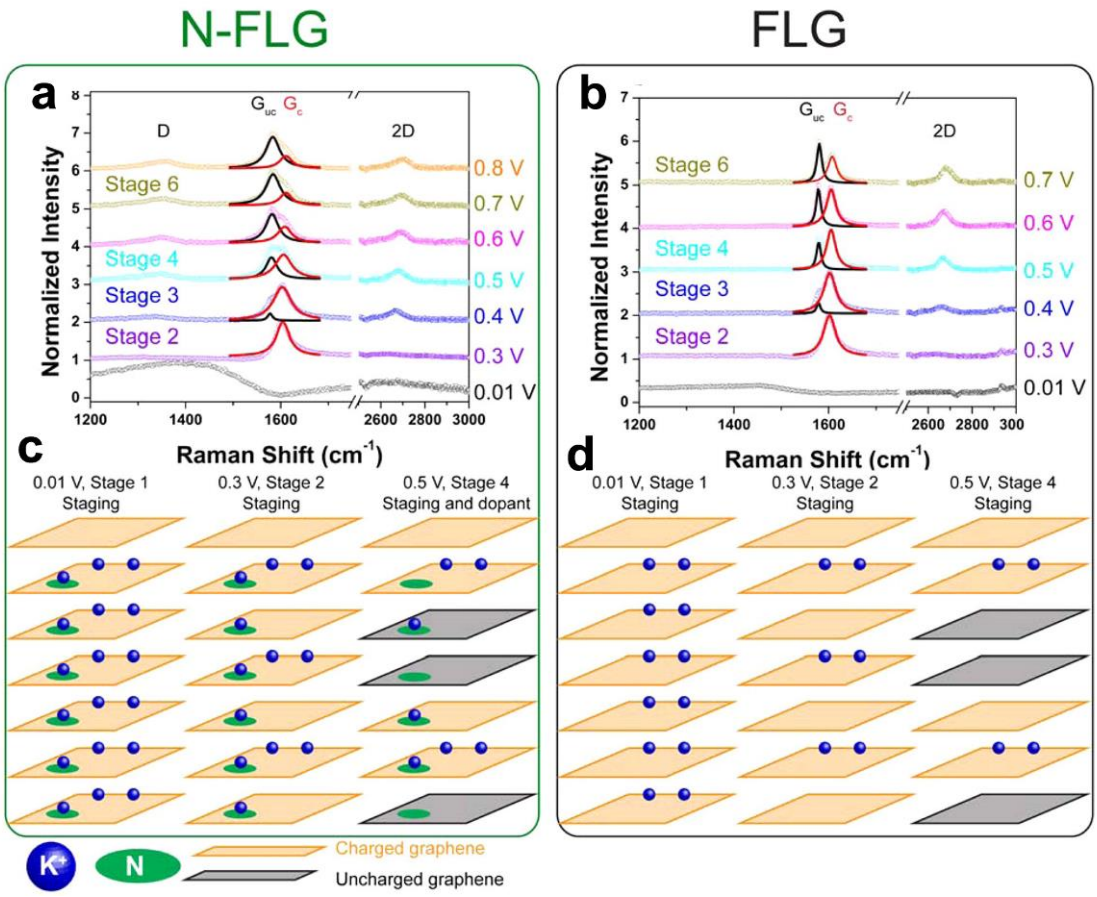

Fig. 4 Raman spectra at selected voltages for N-FLG (a) and FLG (b). Schematic of the staging and defect storage mechanism in N-FLG (c) compared to traditional staging of FLG (d).[36] Copyright 2016, American Chemical Society.

3.2 N-doped Non-graphitic Carbon

Since the potassium storage performance of conventional graphite anode remains unsatisfactory, a variety of amorphous carbon materials have been employed as anodes for PIBs. Particularly, the introducing of N atoms into the carbon materials as an effective strategy is also emphasized. N-doped carbon materials can be synthesized by two primary methods: (i) post-treatment method, *i.e*. making carbon materials react with N-containing reagents (*e.g* ammonia, urea, NO), and (ii) in-situ synthesis methods, namely, thermal decomposition of N-containing precursors. [38]. In this section, we mainly discuss the fabrication of N-doped non-graphitic carbon materials and their electrochemical performances in PIBs.

3.2.1 Post-treatment Method

For the N-doped carbon, the general synthesis method is to import N atoms from external sources, such as NH_3, urea, melamine *etc*. For example, Zhang *et al.* [39] fabricated highly N-

doped porous carbon nanosheets (N-PCNs) through a template-removal and a subsequent annealing process under Ar/NH_3 atmosphere (see Fig. 5). As shown in the XRD pattern, N-PCNs possess larger interlayer distance (0.388 nm) than the commercial graphite (0.335 nm). The enlarged interlayer distance is beneficial for promoting the electrochemical insertion/extraction of K^+. In the Raman spectra, the intensity ratio of D band and G band (I_D/I_G) for N-PCNs is 1.89, larger than that of PCNs (1.56), which indicates a larger amount of disorders and topological defects in N-PCNs thanks to the introducing of N atoms. Moreover, N-doping also increases the surface area from 425.2 m^2 g^{-1} (PCNs) to 848.3 m^2 g^{-1} (N-PCNs). As an anode in PIBs, the N-PCNs electrode displays superior rate property of 127.5 mAh g^{-1} at a current density of 5 A g^{-1} and cycling stability of 151.2 mAh g^{-1} after 10000 cycles at 1 A g^{-1}. The superior performances originate from the ultra-high N-doping (12 at%) and large specific surface area, which can supply plenty of active sites for K^+ insertion/extraction, enhance the electronic conductivity, and also offer efficient electrolyte diffusion paths. Furthermore, to get deep insight into the structure-activity relationship between excellent performance of the N-PCNs electrode in PIBs and the N-doping in N-PCNs, the DFT calculations were performed to evaluate and simulate the effect of N-doping on the absorption capability of K^+ and volume change in N-PCNs. The double-layer graphene model was used to simulate the as-synthesized carbon nanosheets. Pure, pyrrolic-N and pyridinic-N doped double-layer graphene structures are constructed based on the X-ray photoelectron spectroscopy (XPS) result in which two kinds of N-doped sites are detected (*i.e.*, pyrrolic-N and pyridinic-N). The adsorption energies of K^+ on pure, pyrrolic-N doped and pyridinic-N doped double-layer grapheneare -0.98, -1.77 and -1.81 eV, respectively. This indicates that the pyrrolic-N and pyridinic-N doping have significantly stronger K^+ adsorption capability. Meanwhile, the interlayer spacing after K^+ adsorption was also calculated. The result shows the N-PCNs material endows a smaller volume change after potassiation process than PCNs. Finally, N-PCNs also exhibit excellent performances in N-PCNs//potassium Prussian blue nanoparticle (KPB) (N-PCNs//KPB) potassium ion full cell, which demonstrates its great potential for future practical applications.

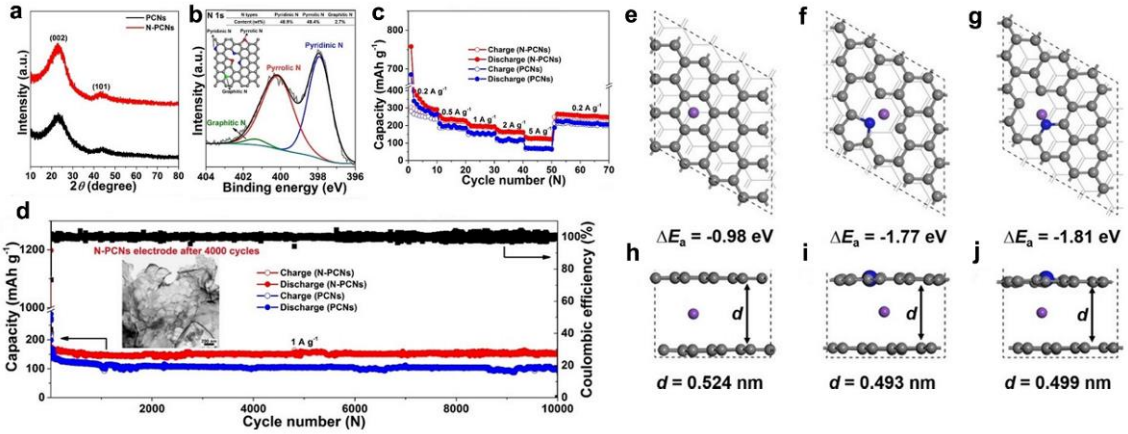

Fig. 5 (a) XRD patterns of N-PCNs and PCNs. (b) High-resolution XPS spectra of N 1s. (c) Rate performance of N-PCNs and PCNs electrodes at different current densities. (d) Cycling performances of N-PCNs and PCNs electrodes with coulombic efficiency of the N-PCNs electrode at 1 A g^{-1}. The inset shows a TEM image of N-PCNs after 4000 cycles. (e-g) Top views and (h-j) side views of K^+ adsorbed on pure, pyrrolic-N doped and pyridinic-N doped double-layer graphene with corresponding adsorption energy values (ΔE_a) and interlayer spacing values (*d*). Grey, blue, and purple balls represent C, N, and K atoms, respectively.[39] Copyright 2020, Wiley.

This method has also been extended to prepare other N-doped carbon materials. Li *et al*. [40] reported hierarchically N-doped porous carbon (NPC) using sodium citrate and urea as raw materials . The NPC electrode delivers high reversible capacity of 384.2 mAh g^{-1} after 500 cycles at a current density of 0.1 A g^{-1} and an outstanding rate capability of 185 mAh g^{-1} at 10 A g^{-1}. The excellent performance can be ascribed to the higher specific surface area and numerous active sites induced by doped N atoms. Wang *et al*. [41] also prepared porous carbon with controllable N-

doping using urea as nitrogen resource. Porous carbon with 12.44 at% N content (NPC-2) delivers a high reversible capacity of 385 mAh g^{-1} at 0.05 A g^{-1}, admirable rate performance of 218 mAh g^{-1} at 2 A g^{-1}, and remarkable long-term cycling stability of 242 mAh g^{-1} after 800 cycles at 0.5 A g^{-1}. These excellent performances are attributed to the appropriate N-doping and porous structure, which not only provide numerous active sites and defects, but also allow the full electrolyte penetration. DFT results also proved that pyridinic-N and pyrrolic-N exhibit higher affinity to K atoms and thus N-doping is beneficial to the K-adsorption on electrode surface. Note that the N doping *via* post-treatment methods usually occurs just on the surface of carbonaceous materials. Thus, the relatively uneven N content in carbon materials usually leads to low yield and high cost, limiting the large-scale production of N-doped carbon materials.

3.2.2 In-situ Synthesis Methods

In addition, N-doped carbon materials can also be obtained by *in-situ* synthesis methods with N-containing carbon precursors. In this section, we mainly introduce the fabrication of N-doped carbon materials synthesized by the carbonization of N-containing precursors, and their electrochemical performances in PIBs, principally from three parts: polymer-derived carbon materials [42], [43], metal-organic frame-works (MOFs) derived carbon materials [44] and biomass-derived carbon materials [45].

Polymer-derived carbon materials

Conducting polymers, such as polyaniline (PANI) [46], [47], polypyrrole [48] (PPy) and polyacryonitrile (PAN) [49], have been employed as carbon precursor and simultaneous nitrogen source. Among them, PANI is one of the most potential conducting polymers and it has been successfully used in supercapacitor electrodes. More importantly, the carbonization of PANI can lead to high-content pyridinic/pyrrolic-N, which is conductive for K-adsorption. For example, Pei *et al*. [50] prepared a series of hollow N-doped carbon nanofibers (HNCNFs) by a facile pyrolysis process with PANI as the precursor (see Fig. 6). The HNCNFs-700 material (HNCNFs annealed at 700 ^{o}C) exhibits an interconnected morphology with a hollow tubular structure. The high-resolution transmission electron microscopy (HRTEM) image demonstrates its disarrayed microstructure. The N content in HNCNFs-700 is calculated to be 8.2 at%. Besides, the HNCNFs-700 possesses higher amounts of pyridinic-N and pyrrolic-N species than that of graphitic-N. As an anode in PIBs, the HNCNF-700 electrode presents an extremely high rate capacity (139.7 mAh g^{-1} at 30 A g^{-1}) and superior long-term cycling stability (188.4 mAh g^{-1} after 4000 cycles at 1 A g^{-1}). The prominent performances can be attributed to the interconnected hollow nanofibers and the high-content pyridinic/pyrrolic N-doping. Moreover, the K-adsorption energies (ΔE_a) at different N-doping sites were calculated on the basis of the DFT simulations. The result indicates that the pyridinic/pyrrolic-N sites have stronger tendencies for K-atom attraction than graphitic-N. Furthermore, the distance between the K atom and pyrindic-N (0.271 nm)/pyrrolic-N sites (0.272 nm) is shorter than that of graphitic-N (0.303 nm), further demonstrating an enhanced affinity of pyrindic-N and pyrrolic-N to K atoms. PPy is another potential conducting polymer, which can also be used as carbon precursor because of its high starting N content. Ruan *et al*. [51] designed high pyridinic N-doped amorphous carbon network (NOCN), which was facilely prepared *via* self-assembly method using PPy as the precursor. The high pyridinic N- and O-doping in the NOCN can effectively introduce abundant detects and unbalanced electron atmosphere, which enhance the K^+ storage quantity and facilitate rapid K^+ insertion/extraction. Besides, the three-dimensional (3D) network structure provides electron channels from one carbon fiber to another, which can enhance the electronic conductivity of NOCN. As a result, the as-synthesized NOCN electrode exhibits an excellent reversible capacity of 464.9 mAh g^{-1} at 0.05 A g^{-1}, outstanding rate performance of 175 mAh g^{-1} at 5 A g^{-1}, and ultra-long cycling performance with capacity decay less than 0.008% per cycle. Combined the post-treatment and *in-situ* synthesis methods, Yang *et al*. [52] fabricated ultra-high pyrrolic/pyridinic N-doped necklace-like hollow carbon (NHC) material as a novel free-standing anode for PIBs. The NHC material was obtained by electrospinning PAN precursor and a subsequent pyrolysis process under NH_3/Ar atmosphere. Thanks to the ultra-high

pyrrolic/pyridinic-N doping, hierarchical micro/meso/macro-pores, necklace-like hollow structure and high specific surface area, the NHC electrode delivers a high reversible specific capacity of 293.5 mA h g^{-1} at 0.1 A g^{-1}, outstanding rate property (204.8 mAh g^{-1} at 2 A g^{-1}) and cycling performance (161.3 mAh g^{-1} at 1 A g^{-1} after 1600 cycles).

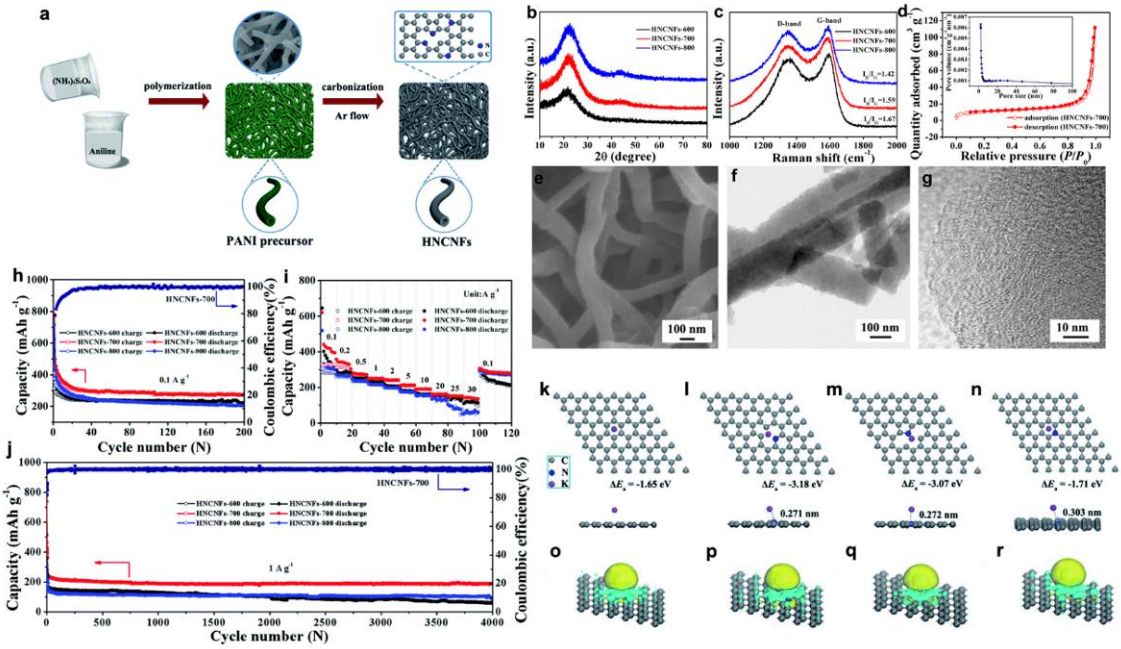

Fig. 6 (a) Schematic illustration of the fabrication process of HNCNFs. (b) XRD patterns of HNCNFs. (c) Raman spectra of HNCNFs. (d) N_2 adsorption/desorption isotherms and pore size distribution (the inset) of HNCNFs-700. (e) FESEM image of HNCNFs-700. (f) TEM and (g) HRTEM images of HNCNFs-700. (h) Cycling performance of the HNCNFs electrodes at 0.1 A g^{-1}. (i) Rate performance of the HNCNFs electrodes at various current densities. (j) Long cycling performance of the HNCNFs electrodes at 1 A g^{-1}. Top and side views of K atom absorbed in the (k) pristine, (l) pyridinic-N, (m) pyrrolic-N and (n) graphitic-N doped carbon structure. Electron density differences of K absorbed in the (o) pristine, (p) pyridinic-N, (q) pyrrolic-N and (r) graphitic-N structures. Blue and yellow areas represent increased and decreased electron density, respectively.[50] Copyright 2020, Royal Society of Chemistry.

MOFs-derived carbon materials

MOFs have been employed as self-templated precursors to obtain N-doped carbon-based materials thanks to high crystallinity and porous characteristics. MOFs comprise two components: an organic linker (the aggregation of numerous molecules) and an inorganic moiety (transition metal ions or small metal clusters) [53]. After calcination steps under inert atmosphere, the organic component can be converted into nanoporous N-doped carbon materials. Yang *et al*. [54] synthesized the N/O dual-doped hierarchical porous hard carbon (NOHPHC) by carbonizing and acidizing the NH_2-MIL-101(Al) precursor (see Fig. 7a). The NOHPHC electrode delivers high reversible capacities of 365 and 118 mAh g^{-1} at 25 and 3000 mA g^{-1}, respectively. When at a high current density of 1050 mA g^{-1}, in the first 300 cycles, the capacity declined from 174 to 130 mAh g^{-1}, but no significant capacity loss the the subsequent cycles. The excellent performance is mainly ascribed to the plentiful surface active sites (N/O dual-doping) and high specific area (about 1030 m^2 g^{-1}).

Zeolitic imidazolate frameworks (ZIFs), another kind of MOF materials, have also been extensively investigated owing to the mild synthesis conditions and flexible synthetic routes. Li *et al*. [55] obtained high pyridinic-N doped porous carbon by annealing ZIF-67 at 600 ^oC (NPC-600) (see Fig. 7b). As the anode material for PIBs, NPC-600 can deliver a high reversible specific capacity (587.6 mA h g^{-1} at 0.05 A g^{-1}), considerable rate properties (186.2 mAh g^{-1} at 2 A g^{-1}) and cycling performance (231.6 mAh g^{-1} at 0.5 A g^{-1} after 2000 cycles). Such excellent electrochemical

performances can be attributed to the increased amounts of pyridinic-N, which provides additional adsorption sites to "capture" more K^+. This simple synthesis approach and unique structure make NPC-600 a promising candidate for PIBs anode. In a similar way, Xu and co-workers [44] reported N-doped carbon nanotubes (NCNTs) using a simple and mild approach of pyrolyzing ZIF-67 (see Fig. 7c). During the pyrolyzing process, the Co nanoparticles can catalyze the organic ligands to grow graphitic CNTs. The as-prepared NCNTs possess hierarchical porous structure with a large surface area of 126 m^2 g^{-1}, which is beneficial for K^+ storage. As a result, the NCNTs electrode delivers a superior rate performance (102 mAh g^{-1} at a current density of 2 A g^{-1}) and an excellent cycling stability (100 mAh g^{-1} after 500 cycles at 2 A g^{-1}). Zhou *et al*. [56] fabricated interconnected N-doped hierarchical porous carbon (N-HPC) by carbonizing ZIF-8 (see Fig. 7d). The 3D bicontinuous porous frameworks reduce the electrons/ions diffusion distance and the N-doping boosts electronic conductivity. Therefore, the N-HPC electrode exhibits a high capacity of 292 mAh g^{-1} at 0.1 A g^{-1}, superb rate capacity of 94 mAh g^{-1} at 10 A g^{-1} and long cycle life (157 mAh g^{-1} for 12000 cycles at 2 A g^{-1}). Compared with other reported carbon materials in PIBs, the advantages of these MOF-derived carbon materials are: (i) the inorganic moiety, for example cobalt, can act as a catalyst to produce carbon materials with various morphology under different conditions, (ii) the N species in ZIF precursors can function as doping heteroatoms in the formation of carbon materials; and (iii) the obtained carbon materials usually possess porous structure with high specific surface area and plentiful surface defects, which can offer numberous active sites, increase the electrode/electrolyte contact area and shorten the ions diffusion distance.

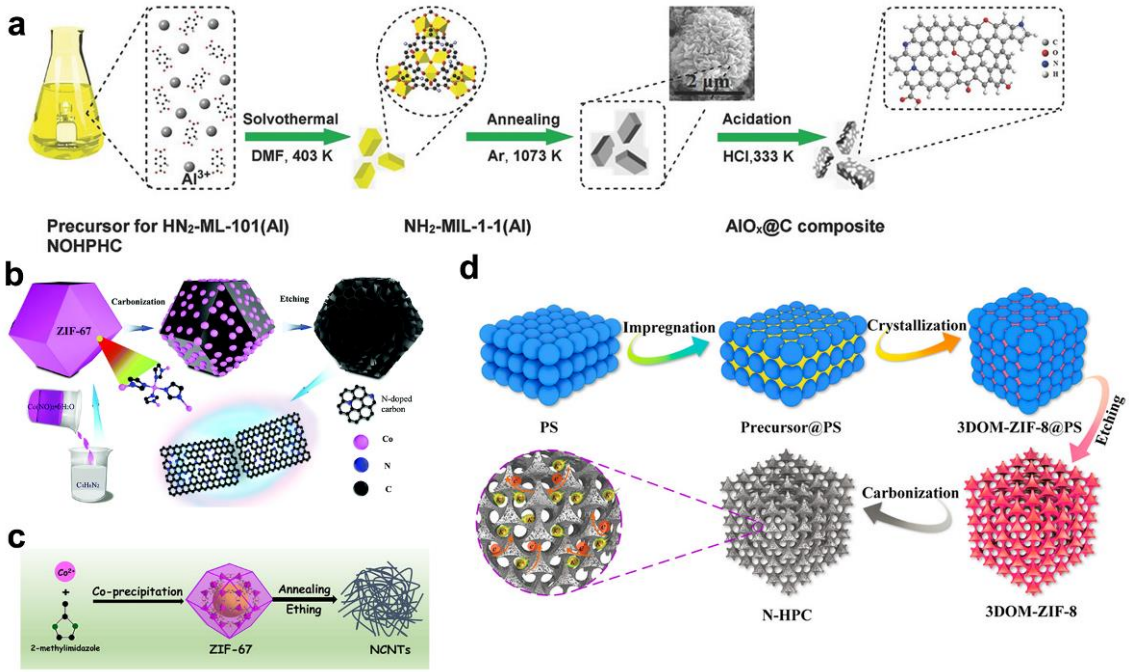

Fig. 7 (a) Schematic illustration of the synthesis of NOHPHC.[54] Copyright 2018, Wiley. (b) The schematic illustration of the fabrication process of NPC materials.[55] Copyright 2018, Royal Society of Chemistry. (c) Schematic illustration of the synthesis of the NCNTs.[44] Copyright 2018, Wiley. (d) Schematic illustration of the synthesis process of N-HPC.[56] Copyright 2019, American Chemical Society.

Biomass-derived carbon materials

Biomass materials are composed of various biopolymers, such as bacterial cellulose [57], bamboo [58], loofah [59], sugar cane [60], pectins [61] and proteins [62], which are in rich of C, H, O and N elementals. After the pyrolysis process, the residual mass turns into amorphous carbons [63]. Biomass-derived carbon used as electrodes for energy storage devices is quite attractive thanks to their advantages of renewable, abundant and low cost [64]. Cui *et al*. [65] constructed

N/O dual-doped hard carbon (NOHC) by carbonizing the renewable piths of sorghum stalks (see Fig. 8). The obtained NOHCs-800 (carbonized at 800 ^{o}C) presents functional groups, hierarchical micro/mesopores structures and abundant active sites. As an anode material for PIBs, NOHCs exhibit a high reversible specific capacity of 304.6 mAh g^{-1} at a current density of 0.1 A g^{-1} over 100 cycles and prominent cycling stability with a capacity of 189.5 mAh g^{-1} at 1 A g^{-1} over 5000 cycles. Moreover, the mechanism during the charge/discharge process of the NOHC-800 electrode was investigated by *ex-situ* HRTEM analysis. The interlayer spacing of NOHC-800 in the initial state is 0.411 nm. After full discharge, it reaches to 0.471 nm, while resumes to 0.422 nm after the full charge. Such a result proves the reversible intercalate/deintercalate of K^{+} in NOHC-800 and its ultra-stable structure. It is apparent that the flexible structure of NOHC-800 can easily adapt to the enlarged interlayer spacing during the discharge process, contributing to superior electrochemical performances of NOHC-800. Moreover, NOHC-800 also exhibits stable cycling property in NOHC-800//KPB potassiation ion full cell. More importantly, NOHC can be applied in large scale, showing great potential for commercialization applications.

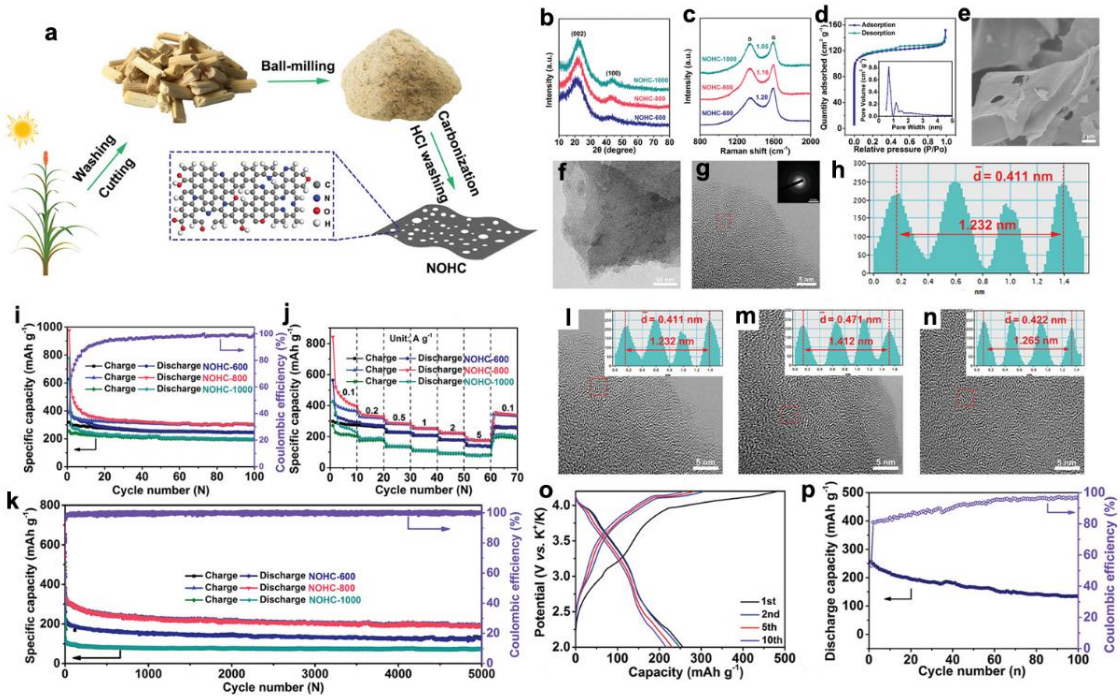

Fig. 8 (a) Schematic illustration of the preparation of NOHC. (b) XRD patterns and (c) Raman spectra of NOHCs. (d) N_2 adsorption-desorption isotherms of NOHC-800. The inset shows the pore size distribution of the adsorption branch obtained by the DFT method. (e-g) FESEM, TEM, and the HRTEM images of NOHC-800. The inset in (g) is a SAED image of NOHC-800. (h) Line profile is acquired from the framed area in (g). (i) Cycling performance of NOHCs at 0.1 A g^{-1}. (j) Rate performance of NOHCs at various current densities. (k) Cycling performance of NOHCs at 1 A g^{-1}. (l-n) *Ex-situ* HRTEM images of NOHC-800 at initial, discharge, and charge states, respectively. (o) Galvanostatic charge/discharge profiles of the NOHC-800//KPB potassium-ion full-cell at 0.1 A g^{-1}. (p) Cycling performance of the full cell at 0.1 A g^{-1}.[65] Copyright 2020, Wiley.

In addition, Zhang *et al*. [66] prepared N, O dual-doped porous carbon (NOPC-750) used corn silk as the precursor. The carbon material doped with N and O atoms possesses larger lattice spacing, leading to lots of electrolyte/ion channels and effective active sites during K^{+} ions insertion/extraction. Employed as a PIBs anode, NOPC-750 presents a high reversible capacity of 309.8 mAh g^{-1} at 0.1 A g^{-1} and excellent rate performance (105.8 mAh g^{-1} even at 20 A g^{-1}). This preparation route provides a low-cost, facile and environmentally friendly solution for yielding high-performance PIBs anode materials. Moreover, Zhang *et al.* [67] designed N/O codoped carbon hollow multihole bowls (CHMBs) synthesized *via* hydrothermal carbonization coupled with

an emulsion-templating strategy using biomass as the carbon source. The CHMBs anode delivers a high reversible capacity of 304 mAh g^{-1} at 0.1 A g^{-1} after 150 cycles and remains a high capacity of 133 mAh g^{-1} over 1000 cycles at 1 A g^{-1}. N/O codopants can produce many edges and surface defects on graphitic layers, which promotes the K^+ adsorption and leads to improved kinetics.

Chitin, one of the most abundant biopolymer in nature, possesses the advantages of low-cost, renewability, natural N-containing functional groups, and intrinsic fibrous structure, showing great superiority over other biomass materials. For instance, chitin-derived hierarchically porous N-doped carbon microsphere (NCS) was developed by Chen *et al*. [68] for the first time. The NCS electrode demonstrates a high rate capability of 154 mAh g^{-1} at 20 A g^{-1} and ultralong cycle life of 4000 cycles without obvious capacity decay (180 mAh g^{-1} at 0.5 A g^{-1}), which is attributed to the hierarchically porous microstructure and N-doped carbon structure with enhanced potassium adsorption capability and electronic/ionic conductivities. Similarly, Hao *et al*. [69] fabricated the N-doped carbon nanofibers (NCFs) by direct pyrolysis of chitin. Specifically, NCFs thermal treated at 700 ^oC exhibit a considerable capacity of 215.2 mAh g^{-1} at 50 mA g^{-1} after 100 cycles, excellent rate capability and cycling stability (105.6 mAh g^{-1} at 0.5 A g^{-1} after 500 cycles). With the spotlight of environmental friendliness, low cost and high energy density in energy storage field, the chitin-based NCFs demonstrate great potential for future low-cost energy storage applications.

4. Conclusions and Prospects

In this review, we summarized recent progress of N-doped carbon anodes for PIBs, which have the merits of low cost, abundant resource and good stability. The potassium storage mechanism of carbon-based materials and the development in the aspects of N-doping were discussed. N-doping is an effective way to enhance electrical conductivity, enlarge surface reaction sites, and generate defect sites and functional groups, resulting in improved specific capacity of carbon materials. Although great progresses have been made, it is always existed that the relatively low Coulombic efficiencies (CEs) for the first several cycles and capacity fading due to the large-sized K^+ insertion/extraction, thus limiting the development of the practical application of PIBs. Therefore, the exploitation of novel anode materials for PIBs is still on the way. Regarding these, some perspectives and outlooks are put forward in the following.

(1) Structural design

In order to mitigate the structural deformation, it becomes desired that engineering different configurations with a capability to tolerate the structural change and to achieve stable electrodes for PIBs. Particularly, designing anode materials with different architectures (such as hollow structures and porous structures) has been considered as an effective strategy to solve the volume expansion problem of electrode materials. For example, hollow structures can significantly improve the cycling stability of the electrode since they can provide an inner space to alleviate the drastic volume change of carbon materials, accordingly alleviating the risk of structural collapse. Porous structures can supply large specific areas to provide sufficient electrolyte penetration, thus facilitating rapid electron/ion transport.

(2) Multi-component doping

Heteroatoms doping (such as N, O, S and P) has been widely applied in carbon materials for PIBs owing to its advantages for enhancing the conductivity, and creating active sites and defects for ion adsorption. Except N element, O-doping can enhance the wettability of the electrolyte. S-doping is also an effective route to improve the potassium storage properties of carbon materials. Thanks to the larger size of S atom, the introducing into carbon can increase the interlayer distance, which not only increases the amount of stored K^+, but also facilitates the rapid K^+ insertion/extraction, finally enhancing the electrode kinetics. For example, Li *et al.* [70] prepared N, S-codoped carbon microboxes (NSC) derived from ZIF-67 *via* an effective carbonization-etching method. Owing to the N (increasing conductivity) and S (enhancing interlayer space) codoped nature, NSC delivers super-long cycle life (180.5 mAh g^{-1} at 500 mA g^{-1} after 1000 cycles) and extraordinary rate property (155.6 mAh g^{-1} at 2 A g^{-1}), which makes NSC a promising anode material for PIBs. Similar to the N, S-doping, P-doping can also enhance the electrochemical performance of carbon materials. He *et al*. [71] successfully obtained high-level pyridinic N-doped

3D honeycomb-liked carbon in conjunction with P doping. The as-obtained P-doped N-rich carbon achieved ultrahigh reversible capacity and outstanding rate capability (419.3 and 270.4 mAh g^{-1} at 100 and 1000 mA g^{-1}, respectively). Therefore, more efforts should be focused on the introducing of other heteroatoms doping or their combinations in carbons materials.

(3) Optimization of electrolytes and binder

The electrolyte plays a critical role in determining the electrochemical performances of PIBs. Generally, the electrolyte contains potassium salts (KPF_6 and KFSI, *etc*.) and alkylene carbonate-based solvents [propylene carbonate (PC), dimethyl carbonate (DMC), ethylene carbonate (EC) and diethyl carbonate (DEC), *etc*.]. The appropriate electrolyte shall ensure the formation of a stable solid electrolyte interphase (SEI) film, which can prevent the exposure of fresh active materials and withstand large volume changes. Additionally, it has been reported that etheryl electrolyte demonstrates a higher initial CE and better cycling stability than carbonate electrolyte owing to the much thinner SEI layers and strong chemical adsorption on the anodes [72], [73]. Moreover, the studies about LIBs and SIBs suggest that the binder also plays an important role in battery performance. Similar phenomenon can also be found in PIBs. For example, Komaba *et al*. [74] reported that the binder selection for the electrode assembly would significantly affect the initial CE and cyclic stability of graphitic anodes in PIBs. However, related investigations about electrolytes and binders are still in the early stage.

(4) Composites design

Other anode materials, such as alloys, metal-based oxides and sulfides, generally have high theoretical capacities. However, they usually suffer from huge volume expansion and possess the nature of poor conductivity. In this regard, designing composites with carbon is an effective method to address these issues. The composites with adaptable network and hierarchical architectures inherite the advantages of the unique metal-based materials and amorphous carbon. Amorphous carbon materials not only use as conductive materials to enhance the conductivity of the composite, but also act as buffers to reduce volume expansion of metal-based nanoparticles.

In summary, to further promote the commercialization of PIBs, it is not enough to reduce the cost just *via* replacing lithium by potassium. Novel, low-cost, compatible and renewable electrodes materials need to be explored and designed. We should also aware that there is still a long way to achieve the practical applications of PIBs for large-scale energy storage.

References

1. *Palomares V., Casas-Cabanas M., Castillo-Martínez E., Han M. H. and Rojo T.,* 'Update on Na-based battery materials. A growing research path', *Energy Environ. Sci., **6** (2013), 2312 – 2337.*
2. *Zhang W., Liu Y. and Guo Z.,* 'Approaching high-performance potassium-ion batteries via advanced design strategies and engineering', *Sci. Adv., **5** (2019), 7412.*
3. *Jing W. T., Yang C. C and Jiang Q.,* 'Recent progress on metallic Sn- and Sb-based anodes for sodium-ion batteries', *J. Mater. Chem. A, **8** (2020), 2913 – 2933*.
4. *Jing W. T., Zhang Y., Gu Y., Zhu Y. F., Yang C. C. and Jiang Q.,* 'N-doped carbon nanonecklaces with encapsulated Sb as a sodium-ion battery anode', *Matter, **1** (2019), 720 – 733*.
5. *Larcher D. and Tarascon J.-M.,* 'Towards greener and more sustainable batteries for electrical energy storage', *Nat. Chem., **7** (2015), 19 – 29.*
6. *Scrosati B., Hassoun J. and Sun Y.-K.,* 'Lithium-ion batteries. A look into the future', *Energy Environ. Sci., **4** (2011), 3287 – 3295*.
7. *Han B., Yang Y., Shi X., Zhang G., Gong L., Xu D., Zeng H., Wang C., Gu M. and Deng Y.,* 'Spontaneous repairing liquid metal/Si nanocomposite as a smart conductive-additive-free anode for lithium-ion battery', *Nano Energy, **50** (2018), 359 – 366.*
8. *Palomares V., Serras P., Villaluenga I., Hueso K. B., Carretero-Gonz´alez J. and Rojo T.,* 'Na-ion batteries, recent advances and present challenges to become low cost energy storage systems', *Energy Environ. Sci., **5** (2012), 5884.*
9. *Dunn B., Kamath H. and Tarascon J.-M.,* 'Electrical energy storage for the grid: a battery of choices', *Science, **334** (2011), 928 – 935*.
10. *Yabuuchi N., Kubota K., Dahbi M. and Komaba S.,* 'Research development on sodium-ion batteries', *Chem. Rev., **114** (2014), 11636.*

11. *Jian Z., Xing Z., Bommier C., Li Z. and Ji X.,* 'Hard carbon microspheres: potassium-ion anode versus sodium-ion anode', *Adv. Energy Mater., **6** (2016), 1501874*.
12. *Kundu D., Adams B. D., Duffort V., Vajargah S. H. and Nazar L. F.,* 'A high-capacity and long-life aqueous rechargeable zinc battery using a metal oxide intercalation cathode', *Nat. Energy, **1** (2016), 16119*.
13. *Yoo H. D., Liang Y., Dong H., Lin J., Wang H., Liu Y., Ma L., Wu T., Li Y. and Ru Q.,* 'Fast kinetics of magnesium monochloride cations in interlayer-expanded titanium disulfide for magnesium rechargeable batteries', *Nat. Commun., **8** (2017), 339.*
14. *Lin M. C., Gong M., Lu B., Wu Y., Wang D. Y., Guan M., Angell M., Chen C., Yang J., Hwang B. J. and Dai H.,* 'An ultrafast rechargeable aluminium-ion battery', *Nature, **520** (2015), 324.*
15. *Chayambuka K., Mulder G., Danilov D. L. and Notten P. H. L.,* 'Sodium-ion battery materials and electrochemical properties reviewed', *Adv. Energy Mater., **8** (2018), 1800079.*
16. *Song K., Liu C., Mi L., Chou S., Chen W. and Shen C.,* 'Recent progress on the alloy-based anode for sodium-ion batteries and potassium-ion batteries', *Small, **15** (2019), 1903194.*
17. *Recham N., Rousse G., Sougrati M. T., Chotard J.-N., Frayret C., Mariyappan S., Melot B. C., Jumas J.-C., and Tarascon J.-M.,* 'Preparation and characterization of a stable $FeSO_4F$-based framework for alkali ion insertion electrodes', *Chem. Mater., **24** (2012), 4363 – 4370.*
18. *Jian Z., Hwang S., Li Z., Hernandez A. S., Wang X., Xing Z., Su D. and Ji X.,* 'Hard-soft composite carbon as a long-cycling and high-rate anode for potassium-ion batteries', *Adv. Funct. Mater., **27** (2017), 1700324.*
19. *Wen Y., He K., Zhu Y., Han F., Xu Y., Matsuda I., Ishii Y., Cumings J. and Wang C.,* 'Expanded graphite as superior anode for sodium-ion batteries', *Nat. Commun., **5** (2014), 4033*.
20. *Okoshi M., Yamada Y., Komaba S., Yamada A. and Nakai H.,* 'Theoretical analysis of interactions between potassium ions and organic electrolyte solvents: a comparison with lithium, sodium, and magnesium ions', *J. Electrochem. Soc., **164** (2017), A54*.
21. *Liu Y., Tai Z., Zhang J., Pang W. K., Zhang Q., Feng H., Konstantinov K., Guo Z. and Liu H. K.,* 'Boosting potassium-ion batteries by few-layered composite anodes prepared *via* solution-triggered one-step shear exfoliation', *Nat. Commun., **9** (2018), 3645*.
22. *Wang G., Xiong X., Xie D., Lin Z., Zheng J., Zheng F., Li Y., Liu Y., Yang C. and Liu M.,* 'Chemically activated hollow carbon nanospheres as a high-performance anode material for potassium ion batteries', *J. Mater. Chem. A, **6** (2018), 24317 – 24323.*
23. *Hosaka T., Kubota K., Hameed A. S. and Komaba S.,* 'Research development on K-ion batteries', *Chem. Rev., **120** (2020), 6358 – 6466*.
24. *Yang W., Zhou J., Wang S., Wang Z., Lv F., Zhang W., Zhang W., Sun Q. and Guo S.,* 'A three-dimensional carbon framework constructed by N/S co-doped graphene nanosheets with expanded interlayer spacing facilitates potassium ion storage', *ACS Energy Lett., **5** (2020), 1653 – 1661*.
25. *Zhao R., Di H., Hui X., Zhao D., Wang R., Wang C. and Yin L.,* 'Self-assembled Ti_3C_2 MXene and N-rich porous carbon hybrids as superior anodes for high-performance potassium-ion batteries', *Energy Environ. Sci., **13** (2020), 246 – 257*.
26. *Wang J., Wang B., Liu Z., Fan L., Zhang Q., Ding H., Wang L., Yang H., Yu X. and Lu B.,* 'Nature of bimetallic oxide Sb_2MoO_6/rGO anode for high-performance potassium-ion batteries', *Adv. Sci., **6** (2019), 1900904*.
27. *Ma M., Zhang S., Yao Y., Wang H., Huang H., Xu R., Wang J., Zhou X., Yang W., Peng Z., Wu X., Hou Y. and Yu Y.,* 'Heterostructures of 2D molybdenum dichalcogenide on 2D nitrogen-doped carbon: Superior potassium-ion storage and insight into potassium storage mechanism', *Adv. Mater., **32** (2020), 2000958.*
28. *Wang H., Xing Z., Hu Z., Zhang Y., Hu Y., Sun Y., Ju Z. and Zhuang Q.,* 'Sn-based submicron-particles encapsulated in porous reduced graphene oxide network: advanced anodes for high-rate and long life potassium-ion batteries', *Appl. Mater. Today, **15** (2019), 58 – 66.*
29. *Lei K., Wang C., Liu L., Luo Y., Mu C., Li F. and Chen J.,* 'A porous network of bismuth used as the anode material for high-energy-density potassium-ion batteries', *Angew. Chem. Int. Ed., **57** (2018), 4687 – 4691*.
30. *He X.-D., Liu Z.-H., Liao J.-Y., Ding X., Hu Q., Xiao L.-N., Wang S. and Chen C.-H.,* 'A three-dimensional macroporous antimony@carbon composite as a high-performance anode material for potassium-ion batteries', *J. Mater. Chem. A, **7** (2019), 9629 – 9637*.
31. *Zhang W., Mao J., Li S., Chen Z. and Guo Z.,* 'Phosphorus-based alloy materials for advanced potassium-ion battery anode', *J. Am. Chem. Soc., **139** (2017), 3316.*
32. *Rüdorff W. and Schulze E.,* 'Über Alkaligraphitverbindungen', *Z. Anorg. Allg. Chem., **277** (1954), 156.*

33. *Nixon D. E. and Parry G. S.,* 'Formation and structure of the potassium graphites', *J. Phys. D: Appl. Phys.*, ***1*** *(1968), 291*.
34. *Jian Z., Luo W. and Ji X.,* 'Carbon electrodes for K-ion batteries', *J. Am. Chem. Soc.*, ***137*** *(2015), 11566*.
35. *Luo W., Wan J., Ozdemir B., Bao W., Chen Y., Dai J., Lin H., Xu Y., Gu F., Barone V. and Hu L.,* 'Potassium ion batteries with graphitic materials', *Nano Lett.*, ***15*** *(2015), 7671*.
36. *Share K., Cohn A. P., Carter R., Rogers B. and Pint C. L.,* 'Role of nitrogen-doped graphene for improved high-capacity potassium ion battery anodes', *ACS Nano*, ***10*** *(2016), 9738.*
37. *Ju Z., Li P., Ma G., Xing Z., Zhuang Q. and Qian Y.,* 'Few layer nitrogen-doped graphene with highly reversible potassium storage', *Energy Storage Mater.*, ***11*** *(2018), 38.*
38. *Quílez-Bermejo J., González-Gaitán C., Morallón E. and Cazorla-Amorós D.,* 'Effect of carbonization conditions of polyaniline on its catalytic activity towards ORR. Some insights about the nature of the active sites', *Carbon*, ***119*** *(2017), 62 – 71*.
39. *Zhang D. M., Chen Z. W., Bai J., Yang C. C. and Jiang Q.,* 'Highly nitrogen doped porous carbon nanosheets as high-performance anode for potassium-ion batteries', *Batteries&Supercaps*, ***3*** *(2020), 185 – 193.*
40. *Li D., Ren X., Ai Q., Sun Q., Zhu L., Liu Y., Liang Z., Peng R., Si P., Lou J., Feng J. and Ci L.,* 'Facile fabrication of nitrogen-doped porous carbon as superior anode material for potassium-ion batteries', *Adv. Energy Mater.*, ***8*** *(2018), 1802386.*
41. *Wang J., Wang D., Dong K., Hao A., Luo S., Liu Y., Wang Q., Zhang Y. and Wang Z.,* 'Fabrication of porous carbon with controllable nitrogen-doping as anode for high-performance potassium ion batteries', *ChemElectroChem*, ***6*** *(2019), 3699 – 3707.*
42. *Xu Y., Zhang C., Zhou M., Fu Q., Zhao C., Wu M. and Lei Y.,* 'Highly nitrogen doped carbon nanofibers with superior rate capability and cyclability for potassium ion batteries', *Nat. Commun.*, ***9*** *(2018), 1720*.
43. *Moussa M., Al-Batainehb S. A., Losic D. and Dubal D. P.,* 'Engineering of high-performance potassium-ion capacitors using polyaniline-derived N-doped carbon nanotubes anode and laser scribed graphene oxide cathode', *Appl. Mater. Today*, ***16*** *(2019), 425 – 434.*
44. *Xiong P., Zhao X. and Xu Y., 'Nitrogen-doped carbon nanotubes derived from metal-organic frameworks for potassium-ion battery anodes', ChemSusChem*, ***11*** *(2018), 202.*
45. *Lin C., Wang Y., Zhong F., Yu H., Yan Y. and Wu S.,* 'Carbon materials for high-performance potassium-ion energy-storage devices', *Chem. Eng. J.*, ***407*** *(2021), 126991*.
46. *Hou L. R., Lian L., Li D. K., Pang G., Li J. F., Zhang X. G., Xiong S. L. and Yuan C. Z.,* 'Mesoporous N-containing carbon nanosheets towards high-performance electrochemical capacitors', *Carbon*, ***64*** *(2013), 141 – 149.*
47. *Fan H. S., Wang H., Zhao N., Xu J. and Pan F.,* 'Nano-porous architecture of N-doped carbon nanorods grown on graphene to enable synergetic effects of supercapacitance', *Sci. Rep.*, ***4*** *(2014), 7426.*
48. *Qie L., Chen W. M., Xu H. H., Xiong X. Q., Jiang Y., Zou F., Hu X. L., Xin Y., Zhang Z. L. and Huang Y.,* 'Synthesis of functionalized 3D hierarchical porous carbon for high-performance supercapacitors', *Energy Environ. Sci.*, ***6*** *(2013), 2497 – 2504.*
49. *Zhong M., Kim E. K., McGann J. P., Chun S. E., Whitacre J. F., Jaroniec M., Matyjaszewski K. and Kowalewski T.,* 'Electrochemically active nitrogen-enriched nanocarbons with well-defined morphology synthesized by pyrolysis of self- assembled block copolymer', *J. Am. Chem. Soc.*, ***134*** *(2012), 14846 – 14857.*
50. *Pei Y. R., Zhao M., Zhou H. Y., Yang C. C. and Jiang Q.,* 'Hollow N-doped carbon nanofibers provide superior potassium-storage performance', *Nanoscale Adv.*, ***2*** *(2020), 4187 – 4198.*
51. *Ruan J., Zhao Y., Luo S., Yuan T., Yang J., Sun D. and Zheng S.,* 'Fast and stable potassium-ion storage achieved by in situ molecular self-assembling N/O dual-doped carbon network', *Energy Storage Mater.*, ***23*** *(2019), 46 – 54.*
52. *Yang W., Zhou J., Wang S., Zhang W., Wang Z., Lv F., Wang K., Sun Q. and Guo S.,* 'Freestanding film made by necklace-like N-doped hollow carbon with hierarchical pores for high-performance potassium-ion storage', *Energy Environ. Sci.*, ***12*** *(2019), 1605 – 1612.*
53. *Jiao L., Seow J. Y. R., Skinner W. S., Wang Z. U. and Jiang H.-L.,* 'Metal-organic frameworks: structures and functional applications', *Mater. Today*, ***27*** *(2019), 43 – 68.*
54. *Yang J., Ju Z., Jiang Y., Xing Z., Xi B., Feng J. and Xiong S.,* 'Enhanced capacity and rate capability of nitrogen/oxygen dual-doped hard carbon in capacitive potassium-ion storage', *Adv. Mater.*, ***30*** *(2018), 1700104.*
55. *Li Y., Yang C., Zheng F., Ou X., Pan Q., Liu Y. and Wang G.,* 'High pyridine N-doped porous carbon derived from metal-organic frameworks for boosting potassium-ion storage', *J. Mater. Chem. A*, ***6*** *(2018), 17959 – 17966.*

56. *Zhou X., Chen L., Zhang W., Wang J., Liu Z., Zeng S., Xu R., Wu Y., Ye S., Feng Y., Cheng X., Peng Z., Li X. and Yu Y.,* 'Three-dimensional ordered macroporous metal-organic framework single crystal-derived nitrogen-doped hierarchical porous carbon for high-performance potassium-ion batteries', *Nano Lett.*, ***19*** *(2019), 4965 – 4973.*
57. *Li H., Cheng Z., Zhang Q., Natan A., Yang Y., Cao D. and Zhu H.,* 'Bacterial-derived, compressible, and hierarchical porous carbon for high-performance potassium-ion batteries', *Nano Lett.,* ***18*** *(2018), 7407 – 7413.*
58. *Tian S., Guan D., Lu J., Zhang Y., Liu T., Zhao X., Yang C. and Nan J.,* 'Synthesis of the electrochemically stable sulfur-doped bamboo charcoal as the anode material of potassium-ion batteries', *J. Power Sources,* ***448*** *(2020), 227572.*
59. *Wu Z., Wang L., Huang J., Zou J., Chen S., Cheng H., Jiang C., Gao P. and Niu X.,* 'Loofah-derived carbon as an anode material for potassium ion and lithium ion batteries', *Electrochim. Acta,* ***306*** *(2019), 446 – 453.*
60. *Wang B., Wang Y., Peng Y., Wang X., Wang J. and Zhao J.,* '3-dimensional interconnected framework of N-doped porous carbon based on sugarcane bagasse for application in supercapacitors and lithium ion batteries', *J. Power Sources,* ***390*** *(2018), 186 – 196.*
61. *Dou X., Hasa I., Hekmatfar M., Diemant T., Behm R. J., Buchholz D. and Passerini S.,* 'Pectin, hemicellulose, or lignin? Impact of the biowaste source on the performance of hard carbons for sodium-ion batteries', *ChemSusChem,* ***10*** *(2017), 2668 – 2676.*
62. *An G.-H., Kim H. and Ahn H.-J.,* 'Surface functionalization of nitrogen-doped carbon derived from protein as anode material for lithium storage', *Appl. Sur. Sci.,* ***463*** *(2019), 18 – 26.*
63. *Hou H., Qiu X., Wei W., Zhang Y. and Ji X.,* 'Carbon anode materials for advanced sodium-ion batteries', *Adv. Energy Mater.,* ***7*** *(2017), 1602898.*
64. *Long W., Fang B., Ignaszak A., Wu Z., Wang Y. J. and Wilkinson D.,* 'Biomass-derived nanostructured carbons and their composites as anode materials for lithium ion batteries', *Chem. Soc. Rev.,* ***46*** *(2017), 7176.*
65. *Cui R. C., Xu B., Dong H. J., Yang C. C. and Jiang Q.,* 'N/O dual-doped environment-friendly hard carbon as advanced anode for potassium-ion batteries', *Adv. Sci.,* ***7*** *(2020), 1902547.*
66. *Zhang Y., Zhao R., Li Y., Zhu X., Zhang B., Lang X., Zhao L., Jin B., Zhu Y. and Jiang Q.,* 'Potassium-ion batteries with novel N, O enriched corn silk-derived carbon as anode exhibiting excellent rate performance', *J. Power Sources,* ***481*** *(2021), 228644.*
67. *Zhang Z., Jia B., Liu L., Zhao Y., Wu H., Qin M., Han K., Wang W. A., Xi K., Zhang L., Qi G., Qu X. and Kumar R. V.,* 'Hollow multihole carbon bowls: A stress-release structure design for high-stability and high-volumetric-capacity potassium-ion batteries', *ACS Nano,* ***13*** *(2019), 11363 – 11371.*
68. *Chen C., Wang Z., Zhang B., Miao L., Cai J., Peng L., Huang Y., Jiang J., Huang Y., Zhang L. and Xie J.,* 'Nitrogen-rich hard carbon as a highly durable anode for high-power potassium-ion batteries', *Energy Storage Mater.,* ***8*** *(2017), 161 – 168.*
69. *Hao R., Lan H., Kuang C., Wang H. and Guo L.,* 'Superior potassium storage in chitin-derived natural nitrogen-doped carbon nanofibers', *Carbon,* ***128*** *(2018), 224 – 230.*
70. *Li Y., Zhong W., Yang C., Zheng F., Pan Q., Liu Y., Wang G., Xiong X. and Liu M.,* 'N/S codoped carbon microboxes with expanded interlayer distance toward excellent potassium storage', *Chem. Eng. J.,* ***358*** *(2019), 1147 – 1154.*
71. *He H., Huang D., Tang Y., Wang Q., Ji X., Wang H. and Guo Z.,* 'Tuning nitrogen species in three-dimensional porous carbon via phosphorus doping for ultra-fast potassium storage', *Nano Energy,* ***57*** *(2019), 728 – 736.*
72. *Lei K., Wang C., Liu L., Luo Y., Mu C., Li F. and Chen J.,* 'A porous network of bismuth used as the anode material for high-energy-density potassium-ion batteries', *Angew. Chem. Int. Ed.,* ***57*** *(2018), 4687 – 4691.*
73. *Lei K., Li F., Mu C., Wang J., Zhao Q., Chen C. and Chen J.,* 'High K-storage performance based on the synergy of dipotassium terephthalate and ether-based electrolytes', *Energy Environ. Sci.,* ***10*** *(2017), 552.*
74. *Komaba S., Hasegawa T., Dahbi M. and Kubota K.,* 'Potassium intercalation into graphite to realize high-voltage/high-power potassium-ion batteries and potassium-ion capacitors', *Electrochem. Commun.,* ***60*** *(2015), 172.*